Karst spring recession and classification: efficient, automated methods for both fast and slow flow components

Tunde Olarinoye[1], Tom Gleeson[2], Andreas Hartmann[1,3]

[1]Chair of Hydrological Modeling and Water Resource, University of Freiburg, Germany
[2]Department of Civil Engineering, University of Victoria, BC, Canada
[3]Chair of Groundwater Systems, Technical University Dresden, Germany

Correspondence to: Tunde Olarinoye (tunde.olarinoye@hydmod.uni-freiburg.de)

Abstract.

Analysis of karst spring recession hydrographs is essential for determining hydraulic parameters, geometric characteristics and transfer mechanisms that describe the dynamic nature of karst aquifer systems. The extraction and separation of different fast and slow flow components constituting karst spring recession hydrograph typically involve manual and subjective procedures. This subjectivity introduces bias, while manual procedures can introduce errors to the derived parameters representing the system. To provide an alternative recession extraction procedure that is automated, fully objective, and easy to apply, we modified traditional streamflow extraction methods to identify components relevant for karst spring recession analysis. Mangin's karst-specific recession analysis model was fitted to individual extracted recession segments to determine matrix and conduit recession parameters. We introduced different parameters optimisation approaches to Mangin's model to increase the degree of freedom thereby allowing for more parameters interaction. The modified recession extraction and parameters optimisation approaches were tested on 3 karst springs in different climate conditions. Our results showed that the modified extraction methods are capable of distinguishing different recession components and derived parameters that reasonably represent the analysed karst systems. We recorded an average KGE >0.85 among all recession events simulated by the recession parameters derived from all combinations of recession extraction methods and parameters optimisation approaches. While there are variabilities among parameters estimated by different combinations of extraction methods, optimisation approaches and seasons, we found even much higher variability among individual recession events. We provided suggestions to reduce the uncertainty among individual recession events and raised questions on how to improve confidence in the system's attributes derived from recession parameters.

1 Introduction

Groundwater from karst aquifers are essential water sources globally (Stevanović 2018; Goldscheider et al. 2020). Karst aquifers are characterised by a high degree of heterogeneity and complex flow dynamics resulting from the interplay of conduit and matrix drainage systems (Kiraly 2003; Goldscheider and Drew 2007). Groundwater flow is rapid in the highly-conductive conduit system whereas is several orders of magnitude slower in the less-conductive matrix system (Goldscheider 2015). While both systems have significant storage capacities, the groundwater residence time is longer in the matrix than in the conduit system (Kovács et al. 2005). Several methods including detailed site-specific speleological investigation (Ford and Williams 2007), tracer tests (Goldscheider and Drew 2007; Goldscheider and Neukum 2010), hydrograph analysis (Kovács et al. 2005; Fiorillo 2014) and model ensembles (Fandel et al. 2020) are used to characterise groundwater flow dynamics in karst systems. Aside from hydrograph analysis which usually requires only spring discharge time series data, other methods are either expensive to apply, time consuming or require more input. This, therefore, makes time series analysis a commonly applied method for karst aquifer flow analyses and modeling (Ford and Williams 2007).

Quantitative time series analysis provides a lumped attributes of the karst aquifer system that are rather difficult to directly measure (Kovács et al. 2005). Karst spring recession analysis still remains a vital quantitative time series analysis tool for estimating aquifer parameters and geometric properties (Fiorillo 2011). Discharge from karst springs reflects the complex interplay of conduit and matrix systems and provides insight into the characteristics of the aquifer which sustains the spring (Kovács et al. 2005; Fiorillo 2014). This also provides essential information for flow prediction as the shape of the spring hydrograph reflects variable aquifer responses to different recharge pathways (Ford and Williams 2007). Since the shape of the spring hydrograph describes in an integrated manner how different aquifer storages and processes control the spring flow (Jeannin and Sauter 1998; WMO 2008a), analysing individual recession limbs of spring hydrograph therefore offers extensive understanding of the structural, storage, and behavioral dynamics of the karst system's drainage (Bonacci 1993).

Numerous studies have employed recession analyses of karst spring hydrograph to characterize karst aquifers, evaluate aquifer properties, manage groundwater resources, predict low flow and estimate baseflow parameters (Padilla et al. 1994a; Dewandel et al. 2003; Kovács et al. 2005; Fiorillo 2014). Derived or estimated recession coefficients are also important parameters in karst models for simulating rainfall-discharge (Fleury et al. 2007; Mazzilli et al. 2019) and other process-based modeling (Hartmann et al. 2013, 2014). Unlike porous media, karst systems cannot be represented by one single storage-discharge function (Ford and Williams 2007). They comprise of multiple subsystems of interconnected conduit and matrix reservoirs, each with its own storage-discharge characteristics (Jeannin and Sauter 1998). Recession analysis models specifically developed for karst spring analysis are usually comprised of two (Mangin 1975) or more (Fiorillo 2011; Xu et al. 2018) independent storage-discharge transfer functions to describe drainage characteristics of different reservoirs and simulate recession flows. Dewandel et al. (2003) provide a general overview and main characteristics of commonly used recession models and those specifically applied to karst systems.

Even though recession analysis of spring hydrographs is cheaper in terms of resources required to explore the flow dynamics and geometry of the karst aquifer system, a major challenge in its application is the separation of the slow flow (matrix-dominated) and quick flow (conduit-dominated) components. The most commonly used karst spring hydrograph separation technique is the semi-logarithmic plot that usually reveals two or more segments. At least one of these segments, typically the last, represents linear reservoir drainage and is attributed to the slow flow (matrix) component (Bonacci 1993; Ford and Williams 2007). The other segment represents the quick flow (conduit) component – a times, a third segment representing the mixed component is also identified. However, this approach is visually supervised and subjectively applied thereby resulting in imprecise and inconsistent estimations. The amount of time required for the visual supervision exercise also makes it impractical to apply this approach to a large number of hydrographs or multiple recession curves, especially if individual recession segment analysis is to be considered for parameters estimation.

However, in other fields of hydrology, there are a handful of automated recession extraction methods that have been developed for extracting streamflow recessions (Arciniega-Esparza et al. 2017). These traditional extraction methods aimed to explicitly identify baseflow recession periods by using different statistical indices to detect less variable flow conditions. During baseflow, streamflow is essentially supported by groundwater storage which provides a less variable flow condition. Contributions from runoff and other unregulated sources that produce highly variable flow during quick flow recession are discarded by these extraction routines (Vogel and Kroll 1996; Brutsaert 2008). Although, these methods were developed to extract baseflow recession from stream hydrographs, there is the possibility to adapt them for extracting matrix and conduit flow recessions of karst springs. In addition to identifying the slow flow recession component, such adaptation will focus on recognizing the quick flow component instead of discarding it. But as these methods are based on different statistical indices for identifying the baseflow regime, they perform differently and produce differing recession parameters (Stoelzle et al. 2013; Santos et al. 2019). Therefore, while attempting to modify these routines, it is also important to explore and compare the differences in the estimated recession parameters that would result from adapting these commonly used traditional recession extraction methods.

Following the extraction of recession events, the estimation of recession parameters is done either by analysing the individual recession segment (IRS) or constructing a master recession curve (MRC) from all events. The MRC approach is commonly used in karst hydrology studies to estimate spring recession parameters, though this approach is also considered to be very biased toward long recession events (Jachens et al. 2020). Also, the single parameters' value derived from this approach does not represent the actual dynamic nature and implicit heterogeneity of karst systems. However, parameters derived from IRS analysis better describe the range of the aquifer system dynamics as well as understanding the seasonal controls on recession behaviour (WMO 2008b). While seasonal control on recession has been widely studied in porous media, studies assessing seasonal effects on karst spring recession are still rare. An advantage of the modified extraction methods herein presented in this study is that, it allowed us to employ the IRS analysis for parameter estimation, as well as projecting the analysis along seasonal dimensions.

Hence, this study aims to develop and test a robust and objective method for extracting karst spring recession components as well as determining the parameters associated with the different components of karst drainage systems. Therefore, in this study, we develop an automated karst recession extraction methods that can identify matrix and conduit components of the karst spring recession hydrograph by modifying the traditional streamflow recession extraction routines. We then estimate conduit and matrix recession parameters of the IRS by using the combination of different modified recession extraction methods and parameters optimisation approaches of the karst recession model. We explore the effect of seasonal influences on the karst conduit and matrix recession parameters as well as the aquifer system classification. Finally, the performances of the different combinations of modified extraction methods and karst recession model parameters optimisation approaches were evaluated.

2 Data and Methods

To develop an automatic karst-specific recession extraction and analysis procedure that is objective and applicable to large hydrograph samples, we first explored the applicability of traditional recession extraction procedures originally developed for non-karst streamflow recessions (Vogel and Kroll 1992; Brutsaert 2008; Aksoy and Wittenberg 2011). Then we analysed karst recession parameters using a two-reservoirs parallel drainage recession model (Mangin 1975). In the following subsections, the recession extraction and analysis model, parameters optimisation approaches, as well as the various adaptations and modifications implemented are described. For consistency, we used the terms 'quick flow' for the turbulent flow from highly conductive karst drainage pathways (synonymous with conduit and storm flow) and 'slow flow' for the laminar flow contribution from less conductive fissures and pores (synonymous with matrix, diffuse and base flow) (Atkinson 1977; Larson and Mylroie 2018).

2.1 Adapting streamflow methods to extract matrix and conduit recession components

Three streamflow recession extraction methods (Vogel and Kroll 1992; Brutsaert 2008; Aksoy and Wittenberg 2011), herein called recession extraction methods (REMs) were adapted to extract matrix and conduit recession components (Table 1). To develop an automated base flow recession extraction routine, Vogel and Kroll (1992) firstly smoothened the stream hydrograph using a 3-day moving average. Thereafter, the decreasing segments of the 3-day moving average are selected as the recession hydrographs. Only segments with 10 or more consecutive days are recognised as recession candidates. To exclude surface and storm runoff influence at the beginning of the recession, the first 30% data points of each recession segment are deleted. Additionally, the difference between two consecutive streamflow values must be ≤ 30% for the pairs to be accepted. All recession segments that satisfied these conditions are then accepted as slow flow recessions segments.

In To to objectively determine streamflow recession that is derived purely from a dry or low flow period, Brutsaert (2008) introduced a more strict recession extraction method. For streamflow *Q*, during time *t*, the Brutsaert method eliminates data points with increasing or zero values of *dQ/dt,* as well as points with abrupt *dQ/dt* values. To exclude data points that might be influenced by storm runoff, three data points after a positive or zero *dQ/dt* are removed - in major events, an additional fourth data point is removed. While Brutsaert (2008) did not provide a description for a major event, Stoelzle et al. (2013) applied the Brutsaert method in their study and defined the major events as streamflow values exceeding 30% frequency. Therefore, we used this definition of a major event from Stoelzle et al. (2013) in this study. Furthermore, the Brutsaert method also excludes the last two data points before a positive or zero *dQ/dt* and spurious data points with larger *-dQ/dt* values.

Aksoy & Wittenberg (2011) extracted the baseflow component from the daily streamflow hydrograph during recession by comparing the coefficient of variation (CV) of the recession segment. All days with decreasing or equal observed flowrate are considered as part of the recession curve. Subsequently, a non-linear reservoir model (Eq. 1) is iteratively fitted to the recession curve until the CV is ≤ 0.1. The CV is defined as the ratio of standard deviation between observed flowrates measurements (Q) and calculated flowrate (Qcalc) to the mean of the observed flowrates as expressed by Eq. 2. Segment of the recession curve with the CV ≤ 0.1 is selected as the real baseflow recession, otherwise, the segment is excluded. Only recession curves with 5-day periods or longer are considered. If the number of days becomes less than 5 during iterative curve fitting and CV ≤ 0.1 is not achieved, such a recession event is discarded (Aksoy and Wittenberg 2011). To ensure consistency between the extraction method and the Mangin recession model used in this study (see Section 2.2), the value of b in Eq. 1 is set to 1, thereby making it a linear model.

$$\mathbf{Q_t = Q_0 \left[1 + \frac{(1-b)Q_0^{1-b}}{ab}\right]^{\frac{1}{b-1}}} \qquad (1)$$

$$\mathbf{CV = \sqrt{\frac{n^2}{n-1}\frac{\sum(Q-Q_{calc})^2}{\sum(Q)^2}}} \qquad (2)$$

The three recession extraction approaches (Vogel and Kroll 1992; Brutsaert 2008; Aksoy and Wittenberg 2011) were specifically developed to extract streamflow recessions that are mainly from slow flow contributions. The rules and exclusion criteria specified by each method are aimed at eliminating the quick flow influences from the extracted recession segments. In karst systems, concentrated rapid flow through the conduit networks constitutes the quick flow, while the contribution from slow-velocity drains through the matrix pores constitutes the slow flow. The quick and slow flow represents flows from two different drainage structures and both contribute to the karst spring recession (Fiorillo, 2014; Ford & Williams, 2007; Padilla et al., 1994).

Adapting the streamflow methods for karst spring recession analysis means considering both the slow and quick flow components to model matrix and conduit spring discharges. So, to adapt the traditional REMs, we (i) extracted the spring flow recession curve based on the specific method approach, (ii) attributed the part of the recession curve that satisfied the specified method's exclusion criteria as slow flow (matrix) component, and (iii) assigned the remaining part that is excluded as quick flow (conduit) component. Table 1 provides an overview of the rule-based baseflow recession extraction methods and changes made in adapting them to include the quick flow component of recession.

Table 1: Criteria for recession extraction methods (REMs)

Recession extraction method	General Criteria	Filter	Slow flow selection	Adaptation for quick flow selection
Vogel	Decreasing 3-day moving day average	First 30% days	$Q_t \geq 0.7Q_{t-1}$	First 30% days, $Q_t < 0.7Q_{t-1}$
Brutsaert	$\frac{dQ}{dt} < 0$	First 3 – 4, and last 2 days	$dQ_t/dt < dQ_{(t-1)}/dt$	First 3 or 4 days, $dQ_t/dt > dQ_{(t-1)}/dt$
Aksoy	$\frac{dQ}{dt} \leq 0$	-	CV ≤ 0.10	CV > 0.10

2.2 Karst spring recession analysis

2.2.1 Mangin model

After extraction, we applied Mangin's (1975) recession analysis model which has been widely used for estimating drainage characteristics and aquifer dynamics in fractured non-homogeneous media (Fleury et al. 2007; Liu et al. 2010; Xu et al. 2018; Schuler et al. 2020; Sivelle 2020). To analyse the extracted recessions, we used this method which considers a two-component recession curve by distinguishing between quick flow (mostly through karstic conduits) and slow flow (mostly through the fissure matrix of the carbonate rock) recessions (Figure 1). Mangin presented two equations: Eq.3 describes the linear storage-discharge relationship from the saturated zone during slow flow conditions represented by the Maillet (1905) equation.

$$\mathbf{\phi_t = Q_{r_0}\, e^{-\alpha t}} \qquad (3)$$

where Q_{ro} is the baseflow contribution at the beginning of recession when $t = 0$, α is the recession coefficient with a unit of T^{-1} and t is the lapsed time between discharge at any time t, Q_t and initial discharge at $t = 0$, Q_0; and Eq. 4 describes the non-linear relationship during quick flow recession from the unsaturated zone.

$$\mathbf{\Psi_t = q_0 \frac{1-\eta t}{1+\varepsilon t}} \qquad (4)$$

where q_0 is the difference between Q_0 and Q_{ro}, parameter η describes the infiltration rate through the unsaturated zone. The parameter is defined as $1/t_i$ for the duration of quick flow recession between $t = 0$ and $t_i = 1/\eta$. ε in T^{-1} unit describes the regulating capacity of the unsaturated zone during infiltration and characterises the importance of concavity of quick flow recession (Padilla et al. 1994). The algebraic sum of Eq. 3 and 4 gives Eq. 5, which defines the discharge at time t during the recession period.

$$Q_t = \mathbf{\phi_t + \Psi_t} \qquad (5)$$

Since t_i is the point of intersection of the slow flow and quick flow component of the recession curve and infiltration stopped when $t > t_i$ ($t > 1/\eta$), so the quick flow component ψ_t in Eq. 5 is essentially assumed to be zero at that point ($\psi t = 0$) (Ford and Williams 2007; Civita and Civita 2008). Therefore, the application of Mangin's model requires, firstly fitting the slow flow component ϕ_t, to the slow flow segment of the recession curve using Eq. 3 to determine the recession coefficient α. Afterward, Eq. 5 was fitted to determine the η and ε parameters of the quick flow segment. However, the accuracies of Q_{ro}, t_i, and the linear representativeness of the slow flow component of the recession curve are critical for the reliable estimation of recession coefficients (Ford and Williams 2007).

2.2.2 Mangin classification framework

Following the estimation of recession parameters α, η and ε using Eqs 3 – 5 above, Mangin proposed a classification scheme for karst systems based on two additional parameters: (1) aquifer regulation capacity, K, and (2) infiltration delay, i. To determine K, the dynamic volume, V_{dyn}, which is defined as the volume of water stored in the phreatic zone at the peak discharge time t_0 is calculated using Eq. 6. The average volume of water, V_{ann}, discharged through the spring's outlet over one hydrological year is also calculated. The regulation capacity K, is therefore given by the ratio of V_{dyn} and V_{ann} as expressed with Eq. 7. This parameter represents the extent of the phreatic zone and its ability to regulate groundwater release from storage. While porous aquifers can have values of K > 0.5, a typical karst system is expected to have K < 0.5 (Marsaud 1997; Dubois et al. 2020).

$$V_{dyn} = \frac{Q_{ro}}{\alpha} \qquad \textbf{(6)}$$

$$\boldsymbol{K} = \frac{\boldsymbol{V_{dyn}}}{\boldsymbol{V_{ann}}} \qquad (7)$$

The infiltration delay, i, represents the retardation between infiltration through the unsaturated zone and the spring's outlet. It is calculated as the value of the quick flow component on the second day (t =2) of recession (Eq. 8). The value of i ranges between 0 and 1, where a system characterised by fast infiltration would have a value close to zero and a slow infiltrating system tends towards 1.

$$\boldsymbol{i} = \frac{1-\eta*2}{1+\varepsilon*2} \qquad (8)$$

With the parameters K and i, five classes of karst systems are defined (also see Fig A1): (1) Well developed system (2) Well developed speleological network with large downstream flood plains (3) Upstream karstification with retarded infiltration (4) Complex system and (5) Poorly developed system. Ford and Williams (2007) provided a detailed review of karst aquifer recession analysis and application of the Mangin model.

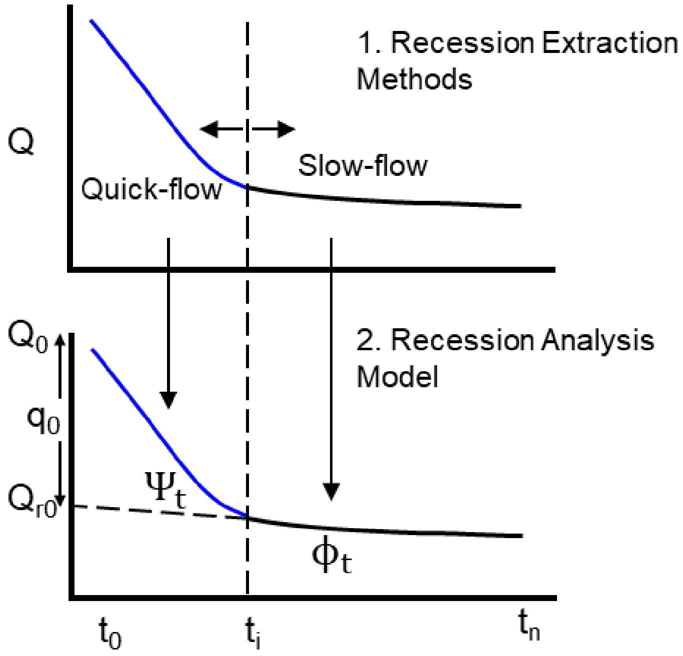

Figure 1. An illustration of karst spring recession curve showing separation into linear and non-linear components by recession extraction method and fitting appropriate components of recession analysis model.

2.3 Estimation of recession parameters

For this study, the parameters were estimated for individual, automatically extracted recession events. That way, we captured the variability of spring discharge across individual recharge events (Jachens et al. 2020). To assess the effects of seasonal variation on the karst spring recession parameters, we separated the extracted events into summer and winter events. For simplicity, events that occurred between April and September of the hydrological year are considered summer events while those from October to March are recognised as winter events. As mentioned in subsection 2.2, in the standard Mangin's approach, the slow flow component of the recession curve (Eq. 3) is fitted at first to determine α. Also, the η parameter of the quick flow component (Eq. 4) which is equivalent to $1/t_i$ is predetermined, meaning that quick flow abruptly ends at t_i days, which cannot be considered optimal. Hence, reliable determination of t_i through the extraction routines (REMs) is vital for estimation of the recession parameters. These standard procedures involved with the application of Mangin's model resulted in less degree of freedom for parameter interaction and unrealistic abrupt ending of quick flow after t_i days. To increase the degree of freedom and assess the importance of t_i and the effect of a priori estimated η ($1/t_i$) on Mangin's recession model, we introduced three optimization approaches, which are referred to as parameters optimisation approaches (POAs) in this study.

- **M1**: This follows the standard approach for applying the Mangin model as described by Padilla et al (1994) and Ford and Williams (2007). The slow flow component of the recession curve is fitted first with Eq. 3 for $t_i \leq t \leq t_n$ to determine the α value while the quick flow component is assumed to be zero during this period. Afterwards, the second parameter ε is optimised by fitting the quick flow component with Eq. 5 using the REM predefined values of η parameter ($\eta = 1/t_i$) for the event duration between $t_0 \leq t < t_i$.

- **M2**: The conventional approach for fitting the Mangin model (M1) does not provide for an independent or flexible estimation of η. The prior definition of η as $1/t_i$ relies on the accuracy of the extraction method to detect the point of inflexion t_i. This however does not give the flexibility to optimise η to a value that can provide a better fit for the model. To provide for a more flexible estimation of η, α parameter is determined as in M1, then Eq. 5 is fitted to the complete segment of the recession curve for $t_0 \leq t \leq t_n$ to determine the best values of ε and η parameters.

- **M3**: This is a very flexible approach that allows for α, ε, η and Q_{ro} values to be fitted numerically. The determination of t_i and Q_{ro} does not depend on the extraction method; rather the best fit for the parameters is obtained from optimisation process. The Mangin model (Eq. 5) is fitted to the entire recession curve, which allowed for absolute flexibility of t_i and robust parameters interaction during optimisation. With the model calibrated t_i ($1/\eta$), separating the quick- and slow flow segments now entirely relies on the optimisation exercise rather than extraction techniques.

For the optimisation exercise, a non-linear least squares procedure with spring discharge records was used. To avoid having a negative value of conduit drainage contribution when the optimised t_i ($1/\eta$) is greater than the elapsing t value, the quick flow component, ψ_t (Eq. 4), was constrained to a minimum value of zero. Table 2 provides summary of the different optimisation approaches, parameters that were optimised as well as the duration of the optimised corresponding flow component.

Table 2: Optimised recession parameters for the three different parameters optimisation approaches (POAs) of the Mangin recession analysis model.

Optim. approach	Optimized parameters	Condition	Slowflow component	Quickflow component	Degree of freedom
M1	α, ε	$\eta = 1/t_i$	$t_i \leq t \leq t_n$	$t_0 \leq t \leq t_i$	Less flexible
M2	α, ε, η	$\eta \neq 1/t_i$	$t_i \leq t \leq t_n$	$t_0 \leq t \leq t_n$	Intermediate
M3	α, ε, η, Q_{ro}	$\eta \neq 1/t_i$	$t_0 \leq t \leq t_n$	$t_0 \leq t \leq t_n$	Very flexible

2.4 Comparison and evaluation of REMs and POAs

The three REMs (Vogel, Brutsaert and Aksoy) were combined with the three POAs (M1, M2 and M3) of the recession model to derive slow and quick flow recession parameters of selected karst springs for a total of nine possible methods. The recession parameters were derived separately for both summer and winter recession events. The overall performance of the different REM and POA combination was determined by calculating the goodness of fit between observed spring recession discharges and ones simulated with the derived parameters using Kling Gupta Efficiency (KGE) measures (Gupta et al. 2009). We used KGE because it considers the common model error types - the mean error, variability and dynamics. The mean and interquartile ranges of the derived parameters were compared among different method pairs and seasons. The estimated recession parameters were used to identify the dynamic of the systems according to Mangin's karst system classification described in subsection 2.2.2. The Mangin classification scheme describes the aquifer drainage characteristics, conduit development and speleological network (Mangin 1975; El-Hakim and Bakalowicz 2007). Therefore, this was used to evaluate the representativeness of recession parameters estimated for the selected karst springs aquifer systems.

3 Test springs and data

The REMs and POAs were tested using three karst springs; Lehnbachquellen, Saivu and Qachquoch located in Austria, Switzerland and Lebanon respectively (Figure 2). The selection of these springs is based on the geographical spread, which covers different climate and hydrological settings, availability of discharge hydrograph in high resolution as well as literature references on the hydrological characterisation of aquifer systems drained by the spring. Daily and sub-daily spring discharge time series of the selected springs were obtained from the WoKaS database (Olarinoye et al. 2020). Important characteristics of the spring hydrographs, as well as the catchments in which they are sited are presented in (Table 3). The springs are sited in catchments distinguished by different climate conditions according to the Köppen-Gieger classification (Beck et al. 2018). Lehnbachquellen is sited in snow-dominated, Saivu is in humid and Qachquoch is in the Mediterranean catchment. It should be noted that in snow catchment, recession behaviour will be externally influenced by snow storage. However, we have included snow-dominated catchment in this study to assess the impact of this external influence. The spring discharge time series was measured at a uniform time step for each spring and spanned between 3 and 13 years. All discharge time series were aggregated to daily temporal resolution, and missing data values which were only found (<0.01%) in Lehnbachquellen spring discharge data were excluded.

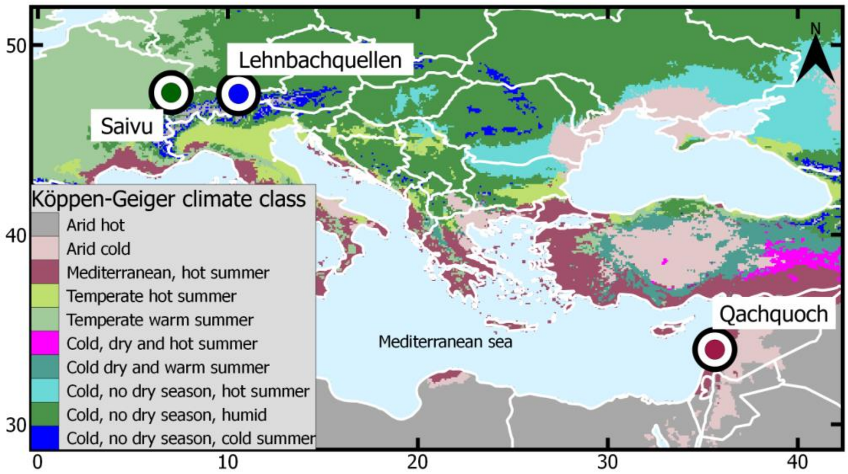

Figure 2. Map showing locations of the three test springs obtained from the WoKaS database and different Köppen-Geiger hydroclimatic classes.

Table 3. Summary of test springs site properties and characteristics of spring discharge hydrographs.

Properties	Lehnbachquellen	Saivu	Qachquoch
Climate description	Snow-dominated	Humid	Mediterranean
Spring elevation (masl)	1293	371	65
Köppen-Geiger	Cold and no dry season	Cold and humid	Mediterranean, hot summer
Temporal res.	Daily	Hourly	Sub-hourly
Length	1999-2012	1993-1995	2014-2018
Missing data	<0.01%	0	0
Mean discharge (m^3/s)	0.06	0.29	1.08
Mean precipitation (mm/y)	1396	1201	523

4 Results

4.1 Extracted recessions and performance of POAs

The adapted recession extraction methods adequately identified karst spring conduit and matrix flow components. The parameters obtained with the different REM-POA pairs also produced satisfactory simulations of recession events. Only complete recession events >= 7 days period were considered for analysis. Here, complete recession referred to events that featured both conduit and matrix components. For each spring hydrograph, a different number of recession events were identified by the REMs. As shown in Table 4, the Vogel method captured the highest number of recession events across all springs, followed by Brutsaert (except for Lehnbacquellen spring) and Aksoy showed the least ability to capture recession periods from the observed spring discharges. However, the average length of the recession events varied among the different REMs in no particular order (see Fig. A2 in appendices). Based on the number of recognizable recession events, the REMs were defined as permissive (Vogel), less permissive (Brutsaert) and restrictive (Aksoy).

Table 4: Recession events period extracted by the REMs for the three spring discharge hydrographs

REM	Lehnbacquellen			Saivu			Qachquoch		
	Total	Summer (%)	Winter (%)	Total	Summer (%)	Winter (%)	Total	Summer (%)	Winter (%)
Vogel	157	0.53	0.47	33	0.42	0.58	41	0.37	0.63
Brutseart	122	0.39	0.61	25	0.48	0.52	36	0.47	0.53
Aksoy	146	0.50	0.50	19	0.58	0.42	31	0.48	0.52

Figure 3 shows how the parameters derived from the different REMs and POAs combinations performed in simulating recession events using the KGE measures. With the exclusion of outliers, a high KGE value is achieved across all combinations, ranging between 0.70 and 1.0. More than half of all simulated events across the three springs produced a KGE >0.9 for all REM-POA pairs. However, the lowest performance in all three springs is related to POAs combined with the Vogel extraction method. While there was no vivid observable pattern among the extraction methods (REMs) and recession model performance, the parameters optimisation approaches (POAs) showed otherwise. A clear systematic order for the KGE median is found within the POAs: M1 < M2 < M3. This is more noticeable in the humid and Mediterranean springs, except for the Vogel-M2 combination in the humid spring, which is not in the systematic order.

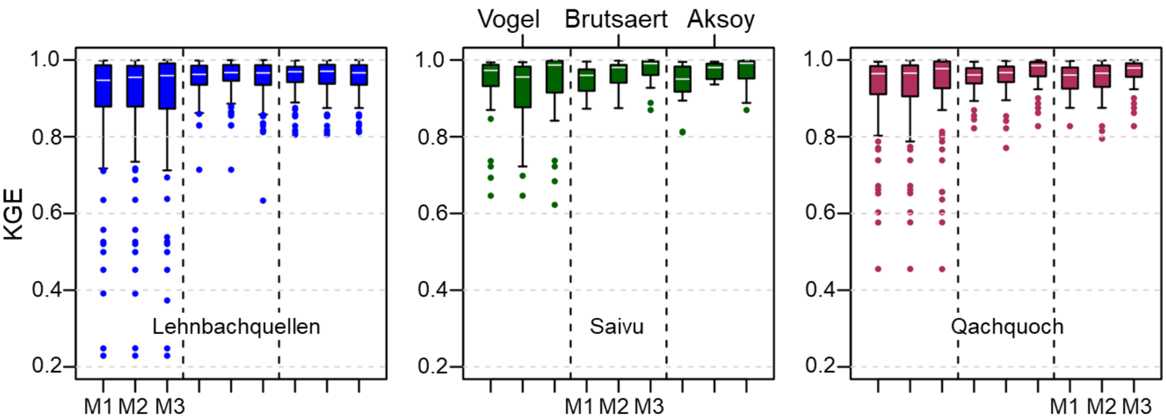

Figure 3: Boxplot of KGE measures between observed and simulated recession events based on parameters derived from the different REMs and POAs. The boxplots represent the interquartile ranges of KGE with the median shown in white lines and outliers marked in coloured points.

4.2 Variability of recession parameters among the different REMs-POAs and seasons

Figure 4 and 5 respectively show the results of the optimised slow flow and quick flow recession parameters for both summer and winter periods. These parameter sets are combinations of α, η and ε that produced the best simulation fit (i.e. highest KGE value) with the different REM-POA pairs. Recession curve fitting based on the individual segment led to a large number of parameter combinations with the nine possible REM-POA pairs. The modification of REMs and POAs produced complex parameter interactions, for simplification, we explored the results along two dimensions: (1) variability among the methods and (2) variability within seasons.

The results from Figure 4 show that REMs and POAs only have marginal effects on the estimation of recession coefficient, α, when compared to the seasonality effect. Also, there are differences in how the REMs and POAs impacted the estimated values of α among the three karst spring catchments. Although, the values of the mean, median and interquartile ranges of α estimated by all the REMs for the snow-dominated catchment seem to be similar, slight differences can still be observed. The slow flow recession parameters estimated by the permissive REM (Vogel) are within slightly higher ranges. On the other hand, the estimation of α in the humid and Mediterranean catchments seems to be more impacted by the POAs. By increasing the degree of freedom of the POAs, higher values of α are estimated, most noticeably with the M3 parameter optimization approach.

While the impacts of methodological approaches (i.e., REMs and POAs) are marginal on the estimated values of α, seasonal impacts on the values and variabilities of the parameter are more evident. The Saivu and Qachquoch springs in humid and Mediterranean catchments respectively showed similar dynamics in terms of seasonal variability of α, while Lehnbacquellen spring located in a snow-dominated catchment showed a different seasonal dynamic. For Lehnbacquellen spring, the values of the estimated α parameter are higher for summer recession events, noticeably with Vogel and Aksoy extraction techniques (Figure 4). During the summer period, estimated α values also showed less variability with Vogel and Brutsaert REMs, while Aksoy gave more varied results for the same season. Meanwhile, an opposite situation is seen with the Saivu and Qachquoch springs. The median values and interquartile ranges of α are higher in winter for estimations done with Vogel and Brutsaert extraction methods. For these springs, estimations associated with the Aksoy extraction method occasionally gave slightly lower α values during winter and less parameter variability. For all the spring systems, the seasonal variability of α is more observable with analysis associated with Vogel, which is the most permissive REM.

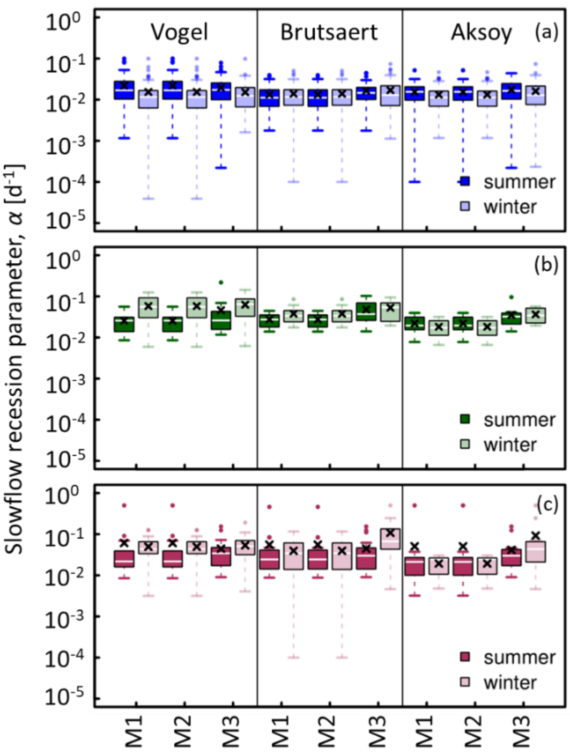

Figure 4. Distribution and variability of slow flow recession parameter, α, obtained by the combination of REM (Vogel, Brutsaert and Aksoy) and POA (M1, M2 and M3) for summer and winter periods: (a) Lehnbacquellen spring in the snow-dominated catchment, (b) Saivu spring located in the humid catchment and (c) Qachquoch spring in the Mediterranean catchment. The boxplots represent the interquartile range, whisker lines correspond to the most extreme parameter values and outliers marked as circles with corresponding box colour.

Both the recession analysis methodology (REMs and POAs) as well as seasons have significant impacts on the estimated values of infiltration rate, η, and curve concavity, ε, parameters. The most visible pattern from Figure 5 is that, the increasing degree of freedom during optimisation usually results in higher estimates (M3 > M2 > M1) and larger variability of η. However, this pattern may slightly vary among the different spring systems. The values of the η parameter spanned one order of magnitude for REMs and POAs combinations across all spring locations. The springs in snow-dominated (Lehnbachquellen) and mediterranean (Qachquoch) catchments showed similar dynamics in terms of seasonal variation of η. The estimated median and mean values of η are higher in winter for both springs. While parameter variability between seasons is relatively comparable in the snow-dominated catchment, larger variability is seen during winter in mediterranean catchment. In the humid catchment, the spring (Saivu) showed an opposite seasonal pattern, summer events have higher η values as well as larger variability.

Estimation of curve concavity parameter, ε, also reflected the influence of recession analysis methods and seasonal variations. The values of ε extend over three orders of magnitude across the three spring locations. In a differing pattern from η, increasing the flexibility of the parametrisation approach (POA) led to low and more consistent ε values. We observed a decreasing order of M1 < M2 < M3 in the estimated values of ε parameter for both summer and winter period. Although, combinations of Brutsaert and Aksoy REMs with most flexible POA (M3) slightly contradicted this order at times, particularly for the humid and mediterranean springs. Although the mean and median values showed slightly higher winter parameter estimations, however, the parameter ranges are similar for both summer and winter periods in the snow-dominated catchment. There is no consistent seasonal pattern in the dynamics of ε estimated for the humid and mediterranean springs. But an understated pattern seen is higher (Saivu spring - humid) or lower (Qachquoch spring – mediterranean) estimations of ε in summer, especially with M1 parameterisation approach.

In general, for the respective seasons, there is relatively better consistency among REM-POA pairs in estimating both slow and quick flow recession parameters as shown by the results in Figure 4 and Figure **5**. In fact, there is much higher parameters variability among recession events than the different REM-POA combinations and seasons.

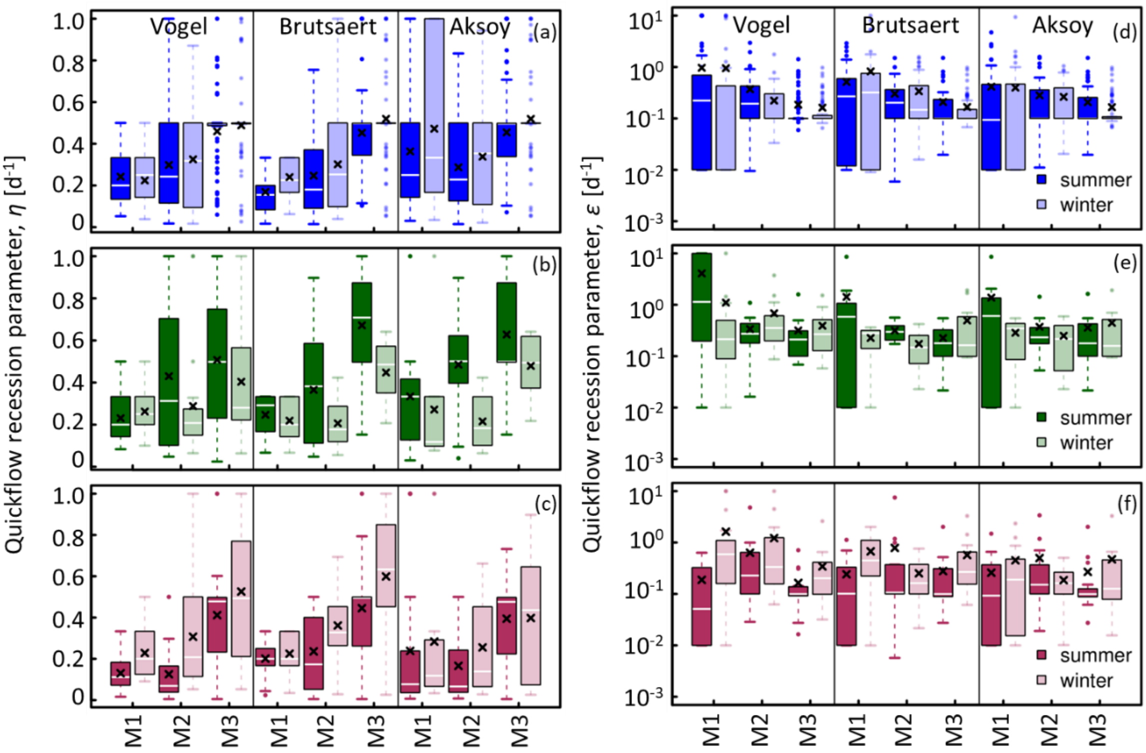

Figure 5. Distribution and variability of the quick flow recession parameters, η and ε, (y-axis of ε in log scale) obtained by the combination of REM (Vogel, Brutsaert and Aksoy) and POA (M1, M2 and M3) for summer and winter periods: (a and d) Lehnbacquellen spring in the snow-dominated catchment, (b and e) Saivu spring located in the humid catchment and (c and f) Qachquoch spring in the Mediterranean catchment. The boxplots represent the interquartile range, whisker lines correspond to the most extreme parameter values and outliers marked as circles with corresponding box colour.

4.3 Aquifer characterization

To evaluate the overall representativeness of estimated recession parameters based on the modified REMs and different POAs for the selected karst spring systems, we determined the drainage properties of the spring's aquifer using the parameters derived from the individual recession event. As described in subsection 2.2.2, retardation between infiltration and output defined by infiltration delay parameter, *i*, and aquifer regulation power, *K*, were calculated for individual recession event. Figure 6 shows the mean aquifer classifications, as well as their standard deviations based on per event estimated *K* and *i* values. The values of *K* and *i* were calculated for individual recession events with the recession parameters derived from the nine REM-POA combinations. As shown by the standard deviation bounds of the drainage properties derived from individual recession segments in Figure 6, there is an overlapping of calculated drainage properties and aquifer classes between the seasons. The methodological differences in the selected REM and POA resulted in large variations in the calculated mean values of infiltration delay, *i*, among the springs. The estimated mean values *i* for the three spring systems used in this study covered similar ranges (0.20 to 0.65). With the exemption of the Lehnbacquellen spring, there was a good coherency in the mean *K* values determined from all combinations of REM and POA for each spring. In addition, the systems are more distinguishable by their ability to store and regulate groundwater outflow through the springs.

Among the three karst springs, only the Qachquoch spring showed a clear impact of seasonality in the system's classification. In summer, the estimated mean *K* values are <0.1 year which is unanimous among the REM-POA combinations. Whereas mean *K* values up to 0.45 and standard deviations of 1.75 years were estimated for the winter recessions. This resulted in a system classification extending from class I (well-developed system) to class IV (complex system) in summer; and a system characterised as predominately class III (fairly karstified system) in winter. Groundwater has a very short residence time in the Saivu spring system for both summer and winter periods. The mean regulation capacity of the system is <0.1 years, although a slightly higher value (ca. 0.15 years) was derived during the winter season. Due to this low regulation power, *K*, of the Saivu spring system, it was characterized predominately as class I in both the summer and winter periods. Only a handful of method combinations placed the system in class III.

While the other two springs (Qachquoch and Saivu) showed either clear or slight seasonal influence in the karst systems characterisation, Lehnbachquellen spring did not show a systematic seasonal impact in its characterisation. Both the estimated mean infiltration delay *i*, and regulation power *K*, showed high inconsistent pattern for Lehnbachquellen spring. The mean *K* values ranged between 0.25 and 0.80 years, with standard deviation values >3 years for both summer and winter recessions events. With these high *K* values, the Lehnbachquellen system has the highest capacity to withhold groundwater among the three karst springs used in this study. The wide dispersion of both *K* and *i* made it impossible to confine the system into a specific class. The Lehnbachquellen system therefore falls within three classes; class II (well-developed system with large downstream flood plains), class III and class V (poorly developed system).

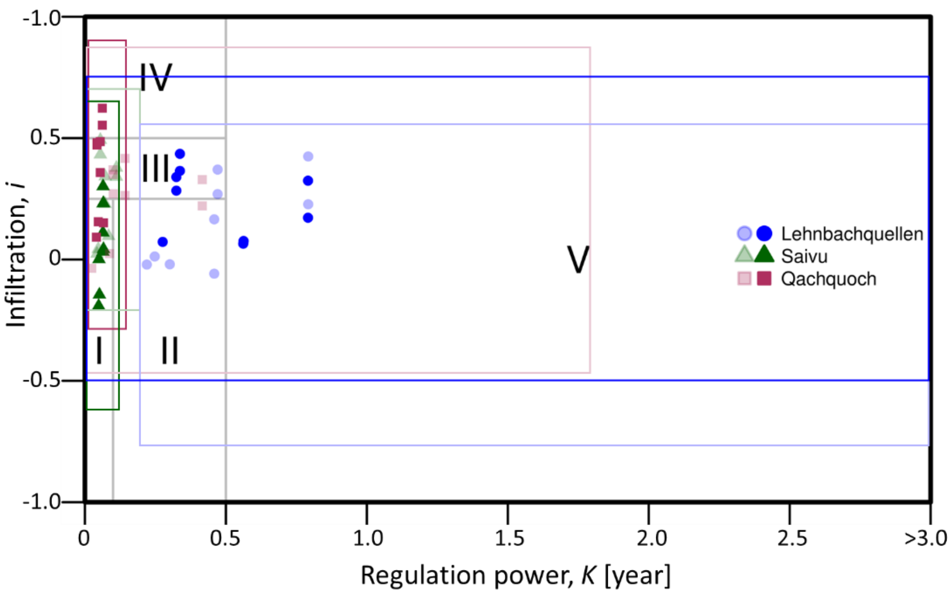

Figure 6. Karst aquifer type classification based on mean values of K and i calculated with recession parameters estimated by the different combinations of REM and POA for both summer (full-shaded colour) and winter (light-shaded colour) periods. Distributions of the per event mean K and i derived from all method combinations for each spring are represented by coloured symbols; areas covered by unfilled boxes are the standard deviations.

5 Discussion

5.1 Quality of extracted recessions

With the modification of the traditional REMs, we were able to establish a completely objective approach to distinguish between slow and quick flow recession components. Furthermore, optimisation approaches (POAs) with more flexibility showed better improvement over the conventional parametrisation procedure. The REMs tested use different empirical approaches to scrutinise genuine baseflow records, hence they have a different levels of tolerance. The ability of the extraction methods to identify recession periods from hydrograph time series depends on the level of their restrictiveness. Vogel extraction method defined by a 3-day moving average to smoothen the hydrograph and also allowed for a 30% increase in subsequent flowrates is more permissive than Brutsaert and Aksoy methods that strictly enforced $dQ/dt < 0$. Hence, more recession events were extracted by the Vogel method. A study by Stoelzle et al. (2013) also showed the Vogel procedure to be more permissive, as it was able to extract almost 50% more events than Brutsaert. Although the main recession selection condition for Brutsaert and Aksoy method is determined by decreasing dQ/dt, constraining real baseflow recessions to discharge data points with less than 10% ($CV \leq 0.1$) deviations makes the Aksoy more restrictive than the Brutsaert method.

Generally, all combinations of REM-POA performed acceptably well, increasing restrictiveness of the extraction method gave an improved model performance. Even though restrictiveness led to better performance, this should not be a basis to out-rightly accept restrictive REM over less-restrictive one. For instance, standard removal of 3 or 4 days by the Brutsaert method as a stormflow-influenced period is speculative and could lead to an unrealistic estimation of conduit flow duration, t_i, ($t_i = 1/\eta$), yet it performed better than the permissive Vogel method. Although, such problem of unrealistic t_i estimation inherent in Brutsaert was eliminated and general improvement in models performances was achieved by increasing parameters flexibility during optimisation. Overall, the adapted REMs and the introduced three POAs provided a range of results that adequately represented the karst systems. However, there are still aspects of automated recession extraction that could benefit from further improvement for their general application in karst hydrology. For instance, the heterogeneous nature of the karst system results in a very dynamic spring discharge pattern, by introducing more tolerance to the REMs to accommodate the usual karst spring discharge anomaly, longer recession events can be extracted. In addition, while all REM-POA pairs are good from the model performance perspective, it will be misleading to define best pair of REM-POA base on this, without evaluating if the estimated parameters are realistic.

5.2 Effects of recession analysis methods and seasonality on extracted recession parameters

5.2.1 Effects of REM-POA combinations on extracted recession parameters

Methodological choices of REMs and POAs combinations have impacts on the estimated recession parameters. The extent to which the parameters are influenced by the methods largely varied between the slow and quick flow recession parameters. There was relatively higher consistency and better stability among all REM-POA pairs in estimating slow flow recession parameters that describe the drainage characteristics of the matrix block within the phreatic zone. Depending on the catchment's hydroclimatic settings, both REMs and POAs showed to have marginal impacts on the estimation of the slow flow recession parameters. Though, this is slightly contrary to other studies that found that slow flow recession coefficients are majorly influenced by the extraction method used, while the parameterization approach only has a marginal impact (e.g. Stoelzle et al. 2013; Santos et al. 2019).

Although the combination of REM and POA affected the estimation of conduit drainage characteristics, the effect of the POA is more pronounced. Increasing the degree of parameter freedom during optimisation with the different POAs formulations often resulted in a significant reduction in the variability of the parameters. This was also accompanied by either low or high estimation of conduit drainage parameters. The more flexible parameterisation approaches (M2 and M3) generally led to higher infiltration rates through the unsaturated zone. The infiltration rate is predetermined ($\eta = 1/t_i$) in the original parameterisation procedure of Mangin's model (M1), therefore restricting the fitting of the quick flow recession curve only to the optimisation of parameter ε, which regulates infiltration through the unsaturated zone. The values of ε smaller than 0.01 have been reported to indicate very slow infiltration and values between 1 and 10 show a domination of fast infiltration (Ford and Williams, 2007; El-Hakim and Bakalowicz, 2007). To compensate for the inflexibility due to the predetermined infiltration rate, the regulation effect of the unsaturated zone was amplified, which is evident in the higher and more varied values of ε estimated with the M1 parameterisation procedure. By means of excluding a fixed number of days (3-4) as the influenced stage of recession, Brutsaert paired with M1 also led to similar values of η estimated for all springs. This makes it an unsuitable combination, especially with a long recession period. In their study, Santos et al. (2019) found analysis with the Brutsaert method to be more robust and appropriate for short recession samples.

Despite the impacts of methodological choices on the uncertainty of estimated recession parameters, variability among events exceeded the variability among methods. These high variabilities are attributed to different lengths of extracted recession events, differences in karstic processes such as recharge, infiltration as well as conduit pathways that are activated within the unsaturated and saturated zones for each event. Even though karst systems are very heterogeneous and it is important to capture the impacts of the variable karstic processes through the analysis of individual recession segments, the high uncertainty among events makes it difficult to define a set of representative recession parameters.

Per event recession analysis is very useful to better understand the karst system dynamics compared to master recession analysis which is unable to depict the hydrodynamic behaviour of karst. However, the high uncertainty found with this approach is still a challenge and a bit difficult to cope with. We believe there are still possibilities for improvement with this approach, for example defining a systematic approach to quantify parameters uncertainties will help to increase the confidence of the individual recession segment analysis.

5.2.2 Seasonal influences on recession parameters

The seasonal variability of slow flow recession parameter is inter-connected with the choice of REM. Among the three different REMs used in this study, a clear seasonal variability of α was more noticeable with Vogel, which is the most permissive REM. However, the observed seasonal variability diminished with increasing restrictiveness of the REM. Also, the pattern of the seasonal variability of α was not the same for all three catchments and this emphasized the influence of climatic controls on karst aquifer drainage. For instance, humid and dry regions are usually characterized by long recession and perhaps a significant drop in groundwater table during summer. From the results presented in the previous section, we identified lower values of α in summer compared to winter. As the parameter α signifies the slope of slow flow recession, a higher value means a steeper slope and faster emptying of the aquifer. The lower α values seen during summer emphasized the drought resistance of the system due decrease in the aquifer hydraulic head. Meanwhile, the snow-dominated catchment showed an opposite behaviour with higher values of α in summer. This occurred due to the accumulation and melting of snow. The snow melting process during the summer period would result in a higher hydraulic head while frozen ice packs in winter translate to a lesser hydraulic gradient. As previously mentioned, a higher hydraulic head would promote faster drainage of the aquifer resulting in higher values of α parameter.

For quick flow recession parameters, seasonal variability is independent of the REM. The three springs showed different seasonal patterns which could be directly linked to their hydroclimatic settings. Seasonal influence on quick flow recession parameters was not clearly seen in the snow-dominated catchment. This could be attributed to the snow melting process discussed above. Since snowmelt compensates for hydrologic flow during warmer periods, there would be a constant influx from the surface throughout the year, also soil wetness conditions would not change significantly. This explains the lack of any evident seasonal differences between parameters η and ε estimated for Lehnbachquellen spring in the snow-dominated catchment. But the Saivu spring in the humid and Qachquoch spring in the mediterranean catchment showed clear seasonal influences. Estimated values of infiltration rates η for Saivu were higher in summer (lower in winter) and lower in summer (higher in winter) for the Qachquoch spring. This pattern is believed to be controlled by the peculiarity of the different geographic and climatic settings. In a humid catchment, higher temperatures in summer would result in dryer soil conditions, which would consequently facilitate faster infiltration. However, for the mediterranean settings, soil conditions are dry due to relatively warmer temperatures all year round. This makes precipitation a limiting factor, and with more precipitation in winter, faster infiltration through the unsaturated zone would occur.

5.3 How realistic are adapted REM-POA for karst system analysis?

Karst system classification proposed by Mangin (1975) is based on two parameters K and i (see subsection 2.2.2). These two parameters were derived from the estimated recession parameters (α, η and ε), thus the variability found in the recession parameters is expected to be propagated to K and i. Although, if the derived mean values of K were considered, some level of coherency was found among all REM-POA combinations and between the seasons. But looking at the estimated standard deviations, a large intra-event and seasonal variation can be found. In a study by Grasso & Jeannin (1994), the authors found regulation power, K, to be more stable for various years and events. These findings did not agree with our analysis, the outcomes of which showed a large variability among K for different events, most significantly in the snow-dominated catchment. Regulation power is analogous to memory effect, and the periodic water release from external snow storage that is not captured within the saturated zone in real-time makes K to fluctuate more in the snow-dominated catchment. Considering the standard deviations from the mean, in fact, the values of K exceeded the maximum value of 1 originally proposed in the Mangin karst classification scheme. Mangin (1975) set a maximum value of one for K, with assumptions that real karst systems would not have a storage memory beyond one year. However, karst system in a snow catchment could have K values greater than one due to snow accumulation and melting as found in Lehnbachquellen spring. Also, complex aquifer systems, as in the case of Qachquoch spring could also have higher K values.

Infiltration delay, i, is strongly dependent on recharge type contribution as well as catchment size (Jeannin and Sauter 1998). Recharge is controlled by climatic input (rainfall) which varies between seasons. However, the derived values of i were hardly separated by season, but more varied among individual recession events. The complex interplay of REM and POA resulted in a compensation phenomenon; whereby infiltration rate, η, was compensated by recession concavity parameter, ε. Since the infiltration delay is defined by these parameters, it is difficult to explicitly infer the specific effects of REM and POA on infiltration delay.

The northern Alps karst system where the Lehnbachquellen spring is located has been defined as well karstified highly permeable unit interlayered with less permeable Flysch formation (Goldscheider 2005; Chen et al. 2018). Our analysis partly placed the karst system in classes II and III thereby showing some consistency with literature evidences. Perrin, Jeannin, &

Zwahlen (2003) described Saivu spring system as a well-developed karstic network, the majority of the methods pair used in this study placed this spring in class 1, therefore coherently agreeing with the authors' description. Taking into account the standard deviations, the classification of Qachquoch spring ranged between medium to poorly karstified system. This is similar to a recent study by Dubois et al. (2020) that categorised the system as poorly karstified with a very large regulation capacity.

Given that the existing common karst spring recession extraction method involves a visually supervised procedure and subjectively determined duration of conduit infiltration, an alternative faster, automated and objective approach is very useful. From our analysis, the resulting parameters of extracted recession segments are within reasonable ranges and the derived systems' classifications correspond to those found in the literature. The good performance recorded between simulated and observed flow rates during recession events attests to the potential transferability of traditional extraction methods to karst systems. However, this good performance does not necessarily translate to reliable parameter estimates. It is therefore important to choose REM methods that give reasonable parameters especially when paired with a less flexible optimisation approach. Furthermore, with prior knowledge of the spring system, parameters ranges can be reasonably constrained during optimisation to achieve more representative optimum parameters.

6 Conclusions

The application of karst spring hydrographs recession analysis is very broad, including estimation of storage capacity (Fleury et al. 2007), describing discharge of unsaturated zone (Amit et al. 2002; Mudarra and Andreo 2011) as well as systems classification (El-Hakim and Bakalowicz 2007). Most often manual recession extraction is used and the high subjectivity of the approach introduced bias to estimated parameters. For the first time in literature, this study explored the applicability of automated traditional recession extraction methods (REMs) originally developed for slow flow (baseflow) recession by adapting them to also identify quick flow recessions. We fitted individual extracted recession segments with Mangin's recession model to determine the conduit and matrix drainages' recession characteristics. We introduce new parameters optimisation approaches (POAs) different from the conventional procedure to increase the degree of freedom of parameter interaction.

While we found that there were uncertainties in the estimated recession parameters resulting from the methodological choices (REM and POA combinations) and seasonal influences, the uncertainties among individual recession events were much larger. The large variability among individual events actually reflected the dynamic heterogeneous nature of the karst system. The combination of this with REMs, POAs and seasons resulted in a more complex interplay and only amplified the uncertainties. These uncertainties are actually useful to understand the dynamic nature karst system, but it is difficult to cope with and also need to be systematically quantified. To avoid these large uncertainties, master recession analysis approach has been a popular alternative for karst spring hydrograph analysis. But a single recession parameters' values derivable from the master recession approach do not reflect the highly dynamic nature of the karst system. The uncertainty of karst recession parameters derived from the either single or master recession approach is presently not a discussion in karst hydrology. Maybe such discussion needs to start to address the limitations and difficulties encountered in this study. Herein, we pose two major issues that need to be addressed as seen in this study: (1) how can we do recession analysis more objectively with a single REM and separation technique that accounts for all ranges and possible instances of slow and quick flow? and (2) how can we incorporate a more robust parameters estimation and uncertainty quantification approach into individual recession analysis? Answering these questions will help to expand confidence in the system's drainage characteristics that are derived from recession parameters.

Finally, this study has shown that there are a lot of potential for extracting and separating karst spring recession components by adapting the traditional REMs and introducing flexible parameter optimization approaches. The adaptation of the REMs in combination with the different parameters estimation flexibility (POAs) provides a suite of automated tools that can be used for karst recession study. This automated and multi approach for parameters optimization is essential to cope with the known biases of single and visually supervised recession analysis methods. Different REM has their specific advantages and there is still room for improvement. For example, other extraction methods can be tested and non-linear reservoir model can also be considered for fitting the matrix model.

*Acknowledgements.*Support to T.O. and A.H was provided by the Emmy Noether Programme of the German Research Foundation (DFG; grant no. HA 8113/1-1; project "Global Assessment of Water Stress in Karst Regions in a Changing World").

Code availability

The R codes for the different REMs and POAs used for the recession analysis can be accessed through our GitHub repository here https://github.com/KarstHub/Karst-recession

References

Aksoy H, Wittenberg H (2011) Nonlinear baseflow recession analysis in watersheds with intermittent streamflow. Hydrol Sci J 56:226–237. https://doi.org/10.1080/02626667.2011.553614

Amit H, Lyakhovsky V, Katz A, et al (2002) Interpretation of Spring Recession Curves. Ground Water 40:543–551. https://doi.org/10.1111/j.1745-6584.2002.tb02539.x

Arciniega-Esparza S, Breña-Naranjo JA, Pedrozo-Acuña A, Appendini CM (2017) HYDRORECESSION: A Matlab toolbox for streamflow recession analysis. Comput Geosci 98:87–92. https://doi.org/10.1016/j.cageo.2016.10.005

Atkinson T. (1977) DIFFUSE FLOW AND CONDUIT FLOW IN LIMESTONE TERRAIN IN THE MENDIP HILLS, SOMERSET (GREAT BRITAIN). J Hydrol 35:93–110

Beck HE, Zimmermann NE, Mcvicar TR, et al (2018) Data Descriptor: Present and future Köppen-Geiger climate classification maps at 1-km resolution. https://doi.org/10.1038/sdata.2018.214

Bonacci O (1993) Karst springs hydrographs as indicators of karst aquifers. Hydrol Sci J 38:51–62. https://doi.org/10.1080/02626669309492639

Brutsaert W (2008) Long-term groundwater storage trends estimated from streamflow records: Climatic perspective. Water Resour Res 44:. https://doi.org/10.1029/2007WR006518

Chen Z, Hartmann A, Wagener T, Goldscheider N (2018) Dynamics of water fluxes and storages in an Alpine karst catchment under current and potential future climate conditions. Hydrol Earth Syst Sci 22:3807–3823. https://doi.org/10.5194/hess-22-3807-2018

Civita M V, Civita M V (2008) An improved method for delineating source protection zones for karst springs based on analysis of recession curve data. Hydrogeol J 16:855–869. https://doi.org/10.1007/s10040-008-0283-4

Dewandel B, Lachassagne P, Bakalowicz M, et al (2003) Evaluation of aquifer thickness by analysing recession hydrographs. Application to the Oman ophiolite hard-rock aquifer. J Hydrol 274:248–269. https://doi.org/10.1016/S0022-1694(02)00418-3

Dubois E, Doummar J, Pistre S, Larocque M (2020) Calibration of a lumped karst system model and application to the Qachqouch karst spring (Lebanon) under climate change conditions. Hydrol Earth Syst Sci 24:4275–4290. https://doi.org/10.5194/hess-24-4275-2020

El-Hakim M, Bakalowicz M (2007) Significance and origin of very large regulating power of some karst aquifers in the Middle East. Implication on karst aquifer classification. J Hydrol 333:329–339. https://doi.org/10.1016/j.jhydrol.2006.09.003

Fandel C, Ferré T, Chen Z, et al (2020) A model ensemble generator to explore structural uncertainty in karst systems with unmapped conduits. Hydrogeol J. https://doi.org/10.1007/s10040-020-02227-6

Fiorillo F (2014) The Recession of Spring Hydrographs, Focused on Karst Aquifers. Water Resour Manag 28:1781–1805. https://doi.org/10.1007/s11269-014-0597-z

Fiorillo F (2011) Tank-reservoir drainage as a simulation of the recession limb of karst spring hydrographs. Hydrogeol J 19:1009–1019. https://doi.org/10.1007/s10040-011-0737-y

Fleury P, Plagnes V, Bakalowicz M (2007) Modelling of the functioning of karst aquifers with a reservoir model: Application to Fontaine de Vaucluse (South of France). J Hydrol 345:38–49. https://doi.org/10.1016/j.jhydrol.2007.07.014

Ford D, Williams P (2007) Karst Hydrogeology and Geomorphology. John Wiley and Sons, Ltd

Goldscheider N (2015) Overview of Methods Applied in Karst Hydrogeology. In: Stevanović Z (ed) Karst Aquifers---

Characterization and Engineering. Springer International Publishing, Cham, pp 127–145

Goldscheider N (2005) Fold structure and underground drainage pattern in the alpine karst system Hochifen-Gottesacker. Eclogae Geol Helv 98:1–17. https://doi.org/10.1007/s00015-005-1143-z

Goldscheider N, Chen Z, Auler AS, et al (2020) Global distribution of carbonate rocks and karst water resources

Goldscheider N, Drew D (2007) Methods in Karst Hydrogeology. International Contributions to Hydrogeology 26, International Association of Hydrogeology. Taylor & Francis, London

Goldscheider N, Neukum C (2010) Fold and fault control on the drainage pattern of a double-karst-aquifer system, winterstaude austrian alps. Acta Carsologica 39:173–186. https://doi.org/10.3986/ac.v39i2.91

Gregor M, Malík P (2012) Construction of master recession curve using genetic algorithms. J Hydrol Hydromechanics 60:3–15. https://doi.org/10.2478/v10098-012-0001-8

Gupta H V., Kling H, Yilmaz KK, Martinez GF (2009) Decomposition of the mean squared error and NSE performance criteria: Implications for improving hydrological modelling. J Hydrol 377:80–91. https://doi.org/10.1016/j.jhydrol.2009.08.003

Hartmann A, Mudarra M, Andreo B, et al (2014) Modeling spatiotemporal impacts of hydroclimatic extremes on groundwater recharge at a Mediterranean karst aquifer. Water Resour Res 1–15. https://doi.org/10.1002/2014WR015685

Hartmann A, Weiler M, Wagener T, et al (2013) Process-based karst modelling to relate hydrodynamic and hydrochemical characteristics to system properties. Hydrol Earth Syst Sci 17:3505–3521. https://doi.org/10.5194/hess-17-3305-2013

Jachens ER, Rupp DE, Roques C, Selker JS (2020) Recession analysis revisited: impacts of climate on parameter estimation. Hydrol Earth Syst Sci 24:1159–1170. https://doi.org/10.5194/hess-24-1159-2020

Jeannin P-Y, Sauter M (1998) Analysis of karst hydrodynamic behaviour using global approaches: a review

Kiraly L (2003) Karstification and Groundwater Flow. Speleogenes Evol karst aquifers 1:155–192

Kovacs A (2021) Quantitative classification of carbonate aquifers based on hydrodynamic behaviour. https://doi.org/10.1007/s10040-020-02285-w

Kovács A, Perrochet P, Király L, Jeannin PY (2005) A quantitative method for the characterisation of karst aquifers based on spring hydrograph analysis. J Hydrol 303:152–164. https://doi.org/10.1016/j.jhydrol.2004.08.023

Kresic N, Bonacci O (2010) Spring discharge hydrograph

Larson EB, Mylroie JE (2018) Diffuse versus conduit flow in coastal karst aquifers: The consequences of Island area and perimeter relationships. Geosci 8:. https://doi.org/10.3390/geosciences8070268

Liu L, Shu L, Chen X, Oromo T (2010) The hydrologic function and behavior of the Houzhai underground river basin, Guizhou Province, southwestern China. Hydrogeol J 18:509–518. https://doi.org/10.1007/s10040-009-0518-z

Maillet E (1905) Essais d’hydraulique souterraine et fluviale. Hermann

Mangin A (1975) Contribution à l’étude hydrodynamique des aquifères karstiques. Institut des Sciences de la Terre de l’Université de Dijon

Marsaud B (1997) Structure et fonctionnement de la zone noyee des karsts a partir des resultats experimentaux

Mazzilli N, Guinot V, Jourde H, et al (2019) KarstMod: A modelling platform for rainfall - discharge analysis and modelling dedicated to karst systems. Environ Model Softw 122:103927. https://doi.org/10.1016/j.envsoft.2017.03.015

Mudarra M, Andreo B (2011) Relative importance of the saturated and the unsaturated zones in the hydrogeological functioning of karst aquifers: The case of Alta Cadena (Southern Spain). J Hydrol 397:263–280. https://doi.org/10.1016/j.jhydrol.2010.12.005

Olarinoye T, Gleeson T, Marx V, et al (2020) Global karst springs hydrograph dataset for research and management of the world’s fastest-flowing groundwater. Sci Data 2020 71 7:1–9. https://doi.org/10.1038/s41597-019-0346-5

Padilla A, Pulido-Bosch A, Mangin A (1994a) Relative Importance of Baseflow and Quickflow from Hydrographs of Karst Spring. Ground Water 32:267–277

Padilla A, Pulido-Bosch A, Mangin A (1994b) Relative Importance of Baseflow and Quickflow from Hydrographs of Karst Spring. Ground Water 32:267–277. https://doi.org/10.1111/j.1745-6584.1994.tb00641.x

Perrin J, Jeannin PY, Zwahlen F (2003) Implications of the spatial variability of infiltration-water chemistry for the investigation of a karst aquifer: A field study at Milandre test site, Swiss Jura. Hydrogeol J 11:673–686. https://doi.org/10.1007/s10040-003-0281-5

Santos AC, Portela MM, Rinaldo A, Schaefli B (2019) Estimation of streamflow recession parameters: New insights from an analytic streamflow distribution model. Hydrol Process 1–15. https://doi.org/10.1002/hyp.13425

Schuler P, Duran L, Johnston P, Gill L (2020) Quantifying and numerically representing recharge and flow components in a karstified carbonate aquifer. Water Resour Res. https://doi.org/10.1029/2020wr027717

Sivelle V (2020) A methodology for the assessment of groundwater resource variability in karst catchments with sparse temporal measurements

Stevanović Z (2018) Global distribution and use of water from karst aquifers. In: Geological Society Special Publication. Geological Society of London, pp 217–236

Stoelzle M, Stahl K, Weiler M (2013) Are streamflow recession characteristics really characteristic? Hydrol Earth Syst Sci 17:817–828. https://doi.org/10.5194/hess-17-817-2013

Vogel RM, Kroll CN (1996) Estimation of Baseflow Recession Constants. Kluwer Academic Publishers

Vogel RM, Kroll CN (1992) Regional geohydrologic-geomorphic relationships for the estimation of low-flow statistics. Water Resour Res 28:2451–2458. https://doi.org/10.1029/92WR01007

WMO (2008a) Manual on Low-flow Estimation and Prediction : Operational Hydrology Report No.50

WMO (2008b) Guide to Meteorological Instruments and Methods of Observation

Xu B, Ye M, Dong S, et al (2018) A New Model for Simulating Spring Discharge Recession and Estimating Effective Porosity of Karst Aquifers A new model for simulating spring discharge recession and estimating e ff ective porosity of karst aquifers. J Hydrol 562:609–622. https://doi.org/10.1016/j.jhydrol.2018.05.039

Appendix

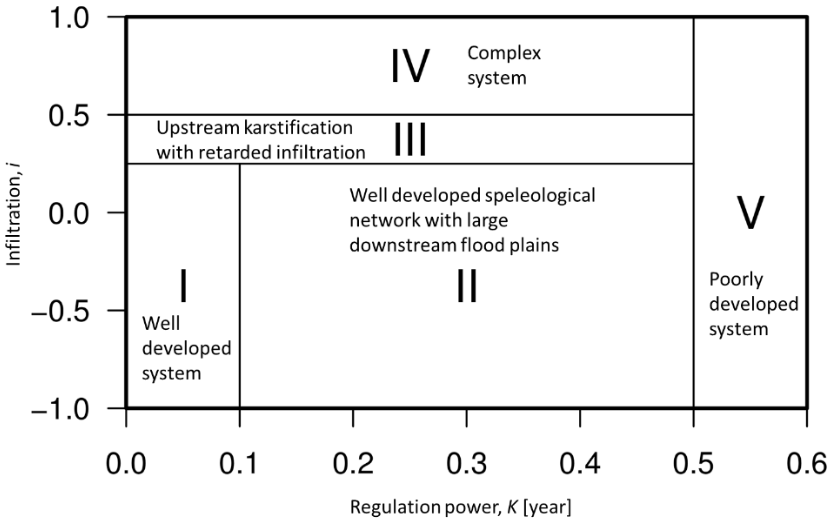

Figure A1. The Mangin (1975) karst system classification scheme based on K and i.

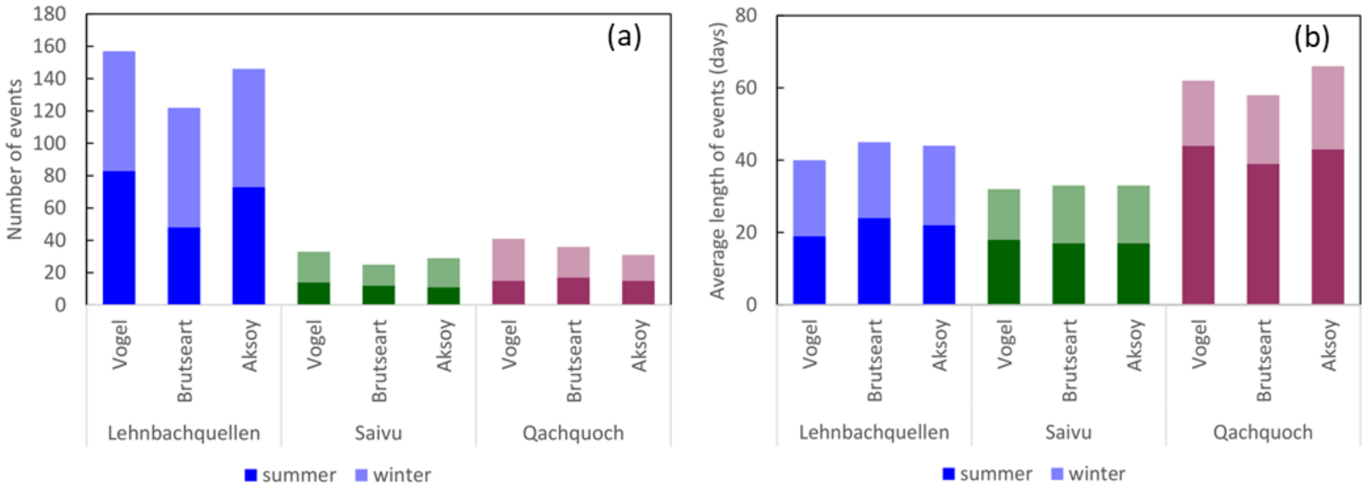

Figure A2. Characteristics of extracted recession events by REMs for both winter and summer periods in the three study sites: (a) number of identified complete recession events, and (b) the average number of days complete recession occurred.

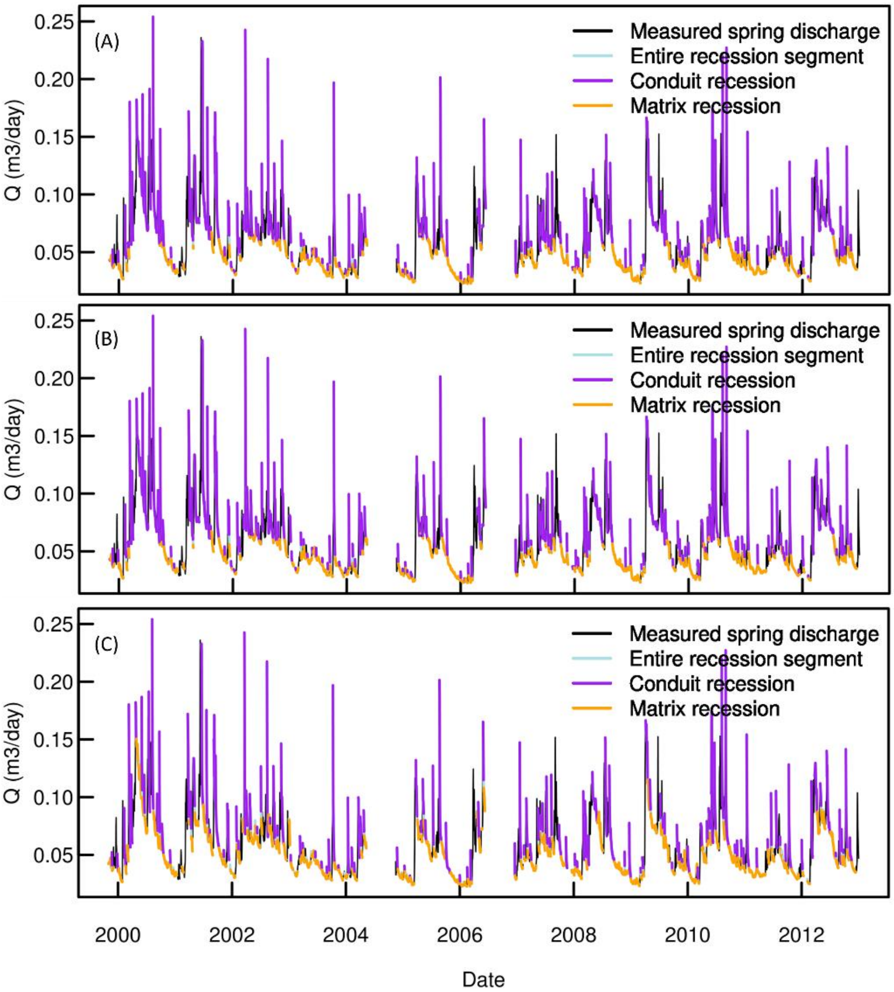

Figure A3. Lehnbachquellen spring discharge hydrograph and extracted recession events recognised by the three REMs: (A) Vogel, (B) Brutseart and (C) Aksoy.

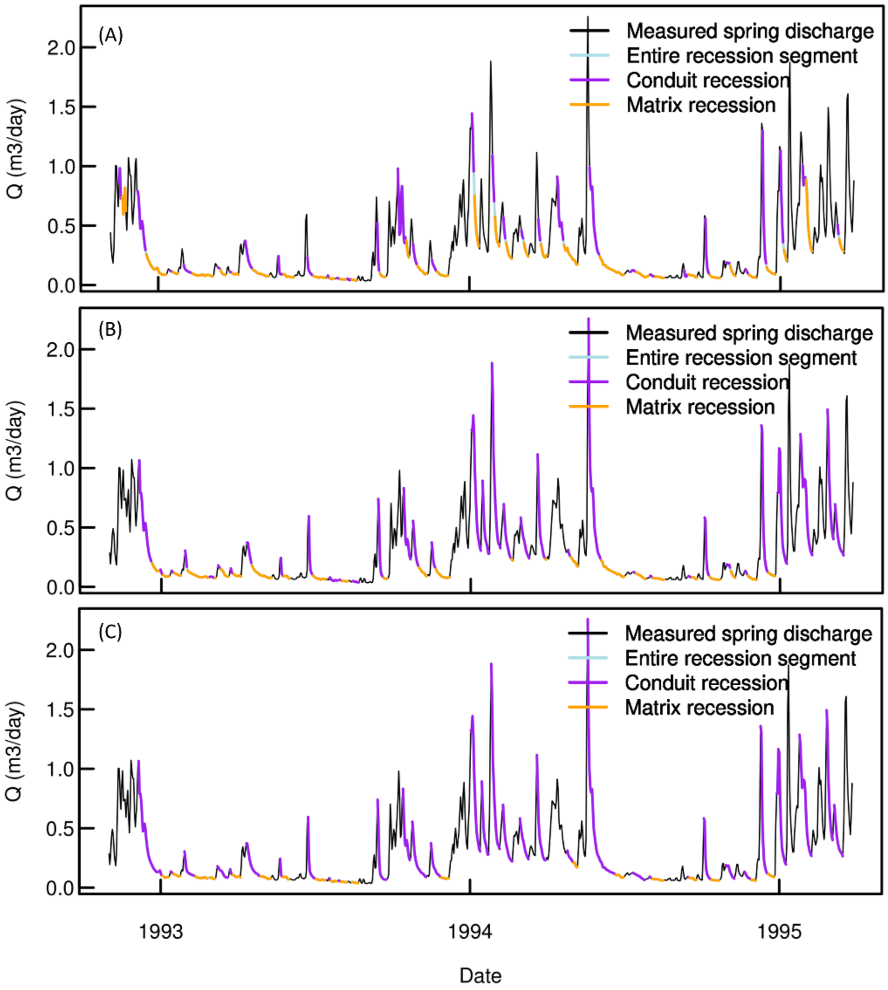

Figure A4. Saivu spring discharge hydrograph and extracted recession events recognised by the three REMs: (A) Vogel, (B) Brutseart and (C) Aksoy.

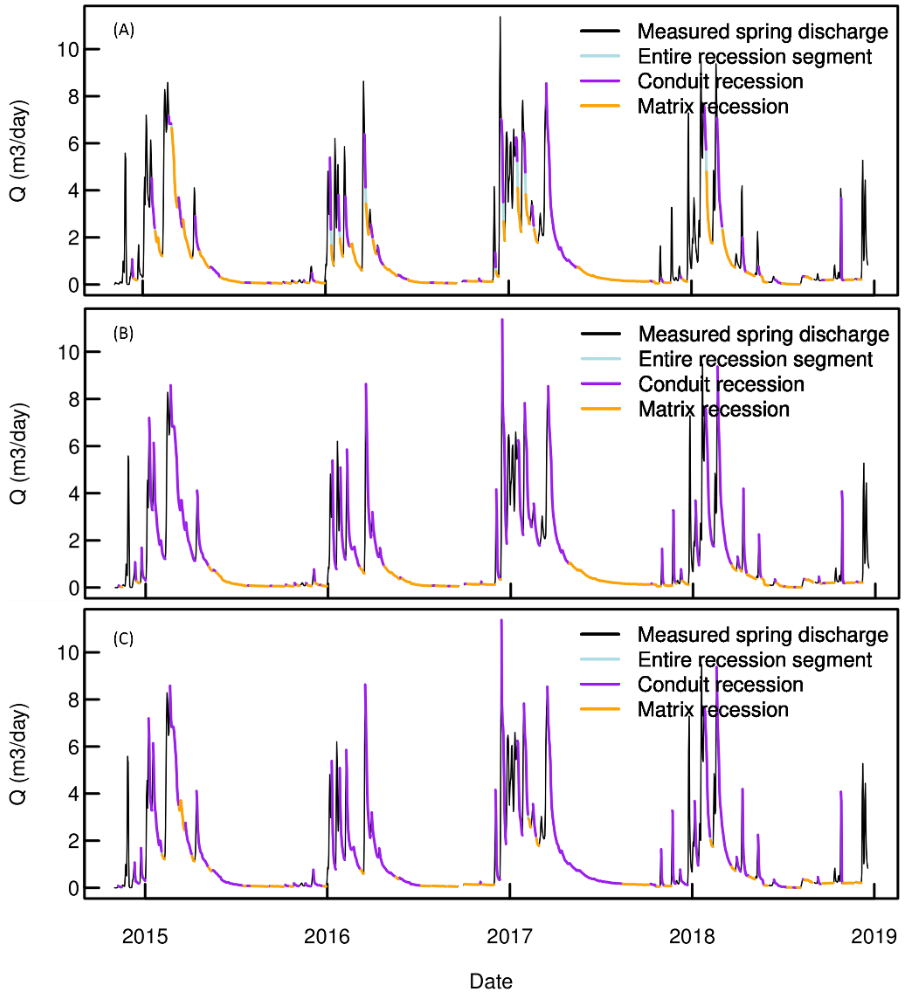

Figure A5. Qachquoch spring discharge hydrograph and extracted recession events recognised by the three REMs: (A) Vogel, (B) Brutseart and (C) Aksoy.